EASR

Engineering and Applied Science Research

https://www.tci-thaijo.org/index.php/easr/index

Published by the Faculty of Engineering, Khon Kaen University, Thailand

Ecological concrete blocks with sawdust additions: Overview of mechanical and microstructural analysis

Sócrates Pedro Muñoz Pérez*[1)], Miriam Gianella Romero Carrasco[2)], Edy Brayan Olivera Espinoza[2)], Juan Martín García Chumacero[2)], Elver Sánchez Diaz[2)], Angel Willian Ocaña Rodriguez[3)], Luigi Italo Villena Zapata[4)] and Ana Paula Bernal Izquierdo[2)]

[1)]Professional School of Civil Engineering, Faculty of Civil Engineering and Architecture, Universidad Cesar Vallejo, Trujillo, Peru
[2)]Professional School of Civil Engineering, Faculty of Engineering and Architecture, Universidad Señor de Sipan, Chiclayo, Peru
[3)]Department of Basic and Related Sciences, Professional School of Civil Engineering, Faculty of Engineering, Universidad Nacional de Barranca, Barranca, Peru
[4)]Professional School of Business Administration, Universidad César Vallejo, Trujillo, Peru

Received 10 September 2024
Revised 15 April 2025
Accepted 7 May 2025

Abstract

Environmental pollution is closely linked to construction practices, especially due to the reliance on non-sustainable materials. This study addresses the scientific challenge of optimizing the sustainability of non-structural concrete blocks through the addition of sawdust, added as a weight-based replacement for sand. The objective was to develop eco-friendly concrete blocks with sawdust to determine their physical, mechanical, and microstructural characteristics. A control sample was prepared, together with four treatments containing sawdust at 5%, 10%, 15% and 20% as a replacement for sand. Tests were conducted to evaluate compressive strength (CR) of individual masonry units, compressive strength of masonry piles, and diagonal shear strength of masonry walls. The results showed that increasing sawdust content led to higher water absorption compared to the control sample. The optimum performance was observed at a 5% sawdust addition, where the compressive strength of piles and the diagonal shear strength of walls increased by 8.59% and 5.51%, respectively. However, compressive strength in masonry units decreased as the sawdust percentage increased. X-ray diffraction (XRD) and scanning electron microscopy (SEM) analyses revealed the presence of crystals such as quartz, calcite, albite, nahcolite, ettringite, cronstedtite, and an amorphous phase, along with chemical elements like carbon, oxygen, silica, and calcium, as well as a slight reduction in voids. The scientific novelty of this study lies in the integration of sawdust as a sustainable additive to improve specific mechanical properties while reducing environmental impact. It is concluded that it is feasible to produce eco-friendly concrete blocks with low sawdust doses that meet the required mechanical standards and exhibit suitable microstructural characteristics. These blocks can be effectively used in non-load-bearing walls and other construction applications where sustainability is a priority.

Keywords: Sawdust, Concrete blocks, Environmental contamination, Mechanical and microstructural characteristics, Masonry units

1. Introduction

Waste generation is increasing in both quantity and variety, encompassing organic and inorganic materials [1]. Inadequate waste management practices are the primary cause of environmental issues, leading to significant ecological challenges [2]. Additionally, industrialization in the late 1990s significantly contributed to increased waste production [3]. The growing global population has intensified the demand for housing, making affordable housing increasingly difficult due to the rising cost of building materials [4, 5]. This demand also drives the extensive use of construction materials like wood, which produces sawdust, a low-density byproduct with heat retention and thermal insulation properties [6-8].

Dawood and Mahmood [9], state that sustainable development concepts can improve both economic welfare and environmental health, however, advancements in greening the masonry materials industry appear limited. Similarly, Kilani et al. [10] also indicate that almost 32 million cubic meters of wood waste and many wood-producing countries generate more than 2 million m^3 of sawdust every year [11], in underdeveloped countries, sawdust is often disposed of by dumping or open burning, practices that generate air pollution, greenhouse gas emissions and degradation of vegetation and aquatic environments [12]. This is supported by Meko and Ighalo [13], who state that sawdust is a by-product of cutting, grinding, drilling, sanding of wood. Additionally, Sharba et al. [14], add that sawdust contributes to a number of environmental difficulties. Each year, increasing amounts of excess sawdust waste are created by manufacturers, sawmills, and real estate activities. In many nations, such as the United States, approximately 64 million tons of wood waste are generated annually.

Opiso et al. [15] highlight sawdust as an eco-friendly alternative to reduce wood industry waste and replace concrete aggregates. The overexploitation of natural sand harms ecosystems, prompting the search for sustainable substitutes. Jeyashree and Somesh [16]

*Corresponding author.
Email address: mperezsp@ucvvirtual.edu.pe
doi: 10.14456/easr.2025.37

emphasize using industrial, agricultural, and household waste to meet rising sand demand. Researching the use of sawdust waste in construction materials is essential as it fosters innovation in sustainable building practices. By exploring new applications for sawdust, a readily available byproduct, we can develop eco-friendly materials that reduce environmental impact [17-21], and promote waste valorization [22-28]. This not only decreases reliance on non-renewable resources but also enhances material properties, such as thermal insulation and lightweight structures [29]. Continuous research drives technological advancements, leading to cost-effective, durable, and energy-efficient construction solutions that support sustainable development goals.

Regarding physical characteristics, Ekhuemelo et al. [30], reduced block density by 4% using 2% sawdust, while Assiamah et al. [31] observed a 7% decrease with 10% sawdust. In contrast, Raheem and Sulaiman [32] achieved only a 1.7% density reduction with 10% sawdust. Shantveerayya et al. [33], using 3% sawdust, reported an 8.03% density reduction compared to the standard block. In another approach, Boob [34], investigated concrete blocks where 5% of the sand was replaced by sawdust, finding that the new block exhibited 412.2% higher water absorption, maintaining a replacement rate of 4%, Abera [35], reported an absorption capacity only 11.1% higher than that of the standard block. The reduction of sawdust and the increase in absorption is due to the fact that sawdust has lower density than the aggregates used for the manufacture of concrete blocks, to an increase in porosity is due to the fact that sawdust tends to create a greater amount of pores in the concrete mix, these pores can be filled with air or water, both with densities much lower than those of solid aggregates. It is important to consider that the reduction in density can also affect the mechanical strength of concrete blocks [36].

Shantveerayya et al. [33], observed a significant 15.38% decrease in compressive strength with 3% sawdust addition compared to a standard block. Abed and Khaleel [37] found an 18.59% reduction with 10% sawdust, and Dominguez-Santos [38] reported a 12.92% decrease, also using 10%. However, conflicting results exist: Dadzie et al. [39] showed a 1.03% strength improvement with 10% sawdust, while Assiamah et al. [31], achieved a 7.5% increase, again with 10% sawdust. Likewise, other mechanical properties such as flexural strength were also studied, where Dominguez-Santos et al. [40], reported an increase in flexural strength of 18.75% with respect to the standard concrete.

X-ray diffraction (XRD) analyses by Muñoz Pérez et al. [17], identified key crystalline phases in concrete, such as silica, portlandite, calcium silicate hydrate, labradorite, dolomite, calcite, hatrurite, gehlenite, ettringite, albite, quartz, orthoclase, aphthitalite, and an amorphous phase [41]. Meena et al. [42] confirmed that these mineral phases contribute to improved concrete strength. Understanding these compositions is crucial for optimizing concrete performance in structural applications. Additionally, microstructural tests by Guo et al. [43] and Adeboje et al. [44] revealed significant variations in elemental composition when incorporating waste materials as aggregate substitutes. Guo et al. reported high levels of carbon (25.68%) and oxygen (33.70%), while Oluwaseun found notable amounts of iron (49%) and chlorine (14.04%) with lower silicon content. Agrawal et al. [45], using energy dispersive spectroscopy (EDS), identified substantial calcium (41.10%) and oxygen (41.15%) concentrations, highlighting the influence of waste materials on concrete's chemical structure and mechanical behavior.

Although previous studies confirm the feasibility of using sawdust in concrete blocks, they are limited by specific experimental conditions, creating a knowledge gap regarding microstructural analysis and compressive behavior of masonry piles. This study introduces the novelty of incorporating sawdust as an additive in ecological concrete blocks at concentrations of 0, 5, 10, 15, and 20%, aiming to evaluate their physical and mechanical properties. The research highlights sawdust's potential as a sustainable alternative to reduce environmental impact. However, limitations include the focus on non-structural applications and the need for further durability assessments under diverse conditions.

2. Materials and methods

2.1 Materials

The aggregates used were fine aggregate and coarse aggregate, which are components of the mix for making concrete blocks. They were subjected to physical tests to characterize the material. It is important to note that the coarse aggregate is referred to as "Confitillo." According to construction regulations, such as the Peruvian National Building Regulations (RNE) and ASTM C33, the fine aggregate (sand) passed through a No. 4 sieve (4.75 mm), and the confitillo had a nominal maximum size of 3/8 inch (9.5 mm), sourced from the Lambayeque region, Peru. As for the cement, Portland Type I cement was used for the investigation, with a density of 3.12 g/cm^3. Table 1 shows the results of the physical characteristics of the aggregates used in the concrete mix and in the Figure 1 shows the flow diagram of the described process.

Table 1 Results of aggregate characterization

Tests	Fine aggregate	Coarse aggregate ("Confitillo")	Standard
Fineness modulus	2.92	-	ASTM C136 [46]
Density (g/cm^3)	2.74	2.71	ASTM C29 [47]
Loose unit weight (kg/m^3)	1526	1201	ASTM C29 [47]
Compacted unit weight (kg/m^3)	1676	1359	ASTM C29 [47]
Absorption (%)	1.52	0.38	ASTM C127 [48]
Moisture content (%)	3.73	1.16	ASTM C566 [49]

The sawdust used in this study was sourced from a sawmill in Lambayeque. It has a density of approximately 250 kg/m³, a moisture content of 12%, and a water absorption capacity of 180%. To ensure uniformity in the concrete mix, the sawdust was sieved to achieve a particle size similar to fine aggregate, passing through No. 4 and No. 16 meshes, allowing optimal distribution within the cement matrix.

No treatment was applied to the sawdust as the objective was to evaluate its natural behavior within the concrete matrix, maintaining its original physical and chemical properties. This approach allows for a realistic assessment of its impact on mechanical performance and durability without additional processing costs. Similar studies Cabanillas et al. [50]; Cadenas et al. [51] have demonstrated that untreated sawdust can still improve thermal insulation and reduce density in eco-friendly concrete applications.

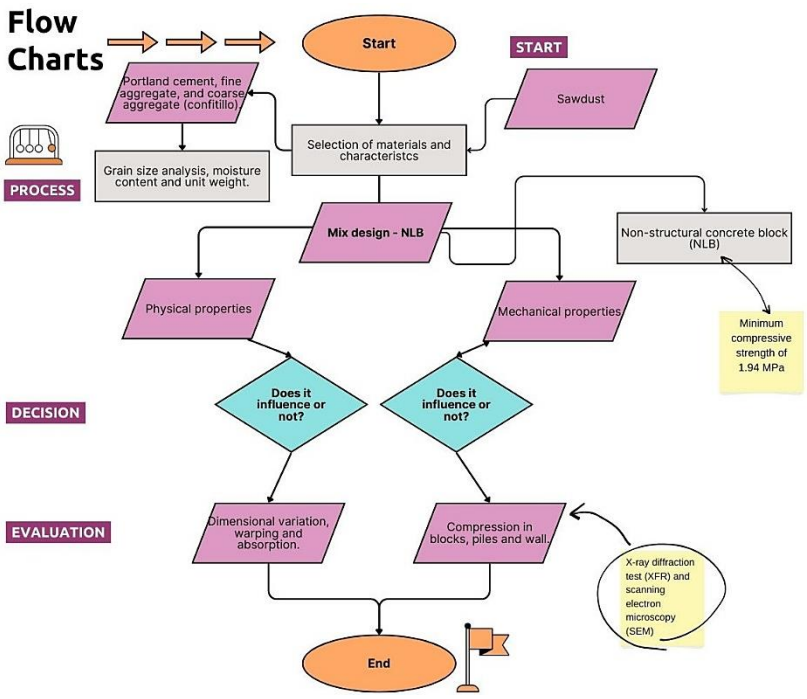

Figure 1 Flow diagram of the present investigation.

2.2 Proportion of materials

A mix for ordinary concrete was designed using the method of Committee 211.1 of the American Concrete Institute (ACI) [52], with a w/c ratio of 0.94. To achieve a minimum compressive strength of 1.94 MPa, corresponding to a non-structural concrete block (NLB), in accordance with the local standard E.070 [53]. Sawdust was added as a replacement by weight in relation to the fine aggregate (sand). The values in Table 2 were expressed in proportional mix ratios (unitless), which represent the relative shares of each material (cement, sand, sawdust and confillo) used in the concrete mix.

Table 2 Dosage of concrete for blocks

Mix design	Cement	Sand	Sawdust	Confitillo
D-1 (Standard block)	1	4.10	0	3.10
D-2 (5% sawdust)	1	4.61	0.24	3.64
D-3 (10% sawdust)	1	4.37	0.49	3.64
D-4 (15% sawdust)	1	4.12	0.73	3.64
D-5 (20% sawdust)	1	3.88	0.97	3.64

2.3 Block making process

The process was calculated and elaborated according to the guidelines of ACI 211.1 [54], for the fabrication of width, height, length (120 x 200 x 400) mm blocks. During the first seven days, when they reach 70% of their maximum strength, the blocks were cured by watering them two or three times a day. On the second day, they were stacked, and the watering process continued for the remaining 28 days. The population for the development of this research was a set of concrete blocks. In the sample there will be 225 hollow concrete blocks; 45 will be normal blocks and 180 containing sawdust.

2.4 Materials testing and methods of analysis

Since the object of the study is to determine the physical, mechanical and microstructural properties of the blocks, making piles and walls, the tests described in Table 3 were carried out. Figure 2 shows the increase in the average resistance of the 5 designs proposed in this research, after subjecting the blocks to compression, the test was carried out on 3 different days, at 7, 14 and 28 days, showing a clear tendency of reduction of the resistance values as the sawdust content in the concrete increases.

Table 3 Test standards for concrete blocks

Test	Dimensions (mm)	International standards
Dimensional variation	120 x 200 x 400	ASTM C140 [55]
Warpage	120 x 200 x 400	ASTM C426 [56]
Absorption	120 x 200 x 400	ASTM C127 [48]
Compressive strength	120 x 200 x 400	ASTM C307 [57]
Compressive strength of masonry prisms	120 x 400 x 400	ASTM C1314 [58]
Diagonal compressive strength of walls	120 x 800 x 800	ASTM E519 [59]

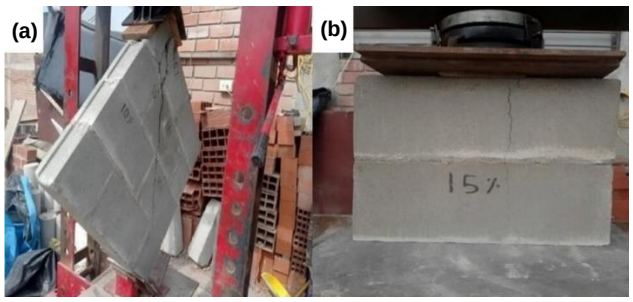

Figure 2 (a) Diagonal compression failure of masonry wall and (b) Vertical failure in masonry prisms.

2.5 Microstructural characteristics

X-Ray Diffraction (XRD) analyses were performed on the supplied samples using a Bruker D8 Focus equipment with copper radiation (CuKα = 0.15418 nm), operating at a current of 40 mA and a voltage of 40 kV, and equipped with a Lynxeye detector with energy selectivity. The analysis was carried out over a range of angles (2θ) from 15° to 70°, with increments of 0.02 degrees and an acquisition time of 1 second per step. To determine the composition of the crystalline phases and the amorphous fraction, the Reference Intensity Ratio (RIR) method was used, which has a minimum detectable concentration of 0.1 wt.%.

Scanning Electron Microscopy (SEM) analysis was carried out using a FEI Quanta 650 microscope, operating at an accelerating voltage of 20 kV and with a spot size of 3. Areas were examined at magnifications of 500X and 2000X. Energy dispersive spectroscopy (EDS) was performed with an EDAX detector integrated in the microscope. Data processing and chemical composition determination were performed using EDAX TEAM software, fitting the spectra and using the eZAF method.

3. Results and discussions

3.1 Physical properties of hollow concrete blocks

3.1.1 Dimensional variation test

According to Figure 3, the ANOVA test yielded a p-value of 0.05791, which is greater than 0.05, indicating no statistically significant differences between treatments. However, treatment D-3 (10% sawdust) exhibited the highest average net sample area, reaching 66.09%. The observed dimensional variations are attributed to the heterogeneous distribution of sawdust particles, which affects compaction and drying behavior. For the standard blocks, dimensional changes were 0.58% (length), 1.79% (width), and 0.74% (height), while for the optimal D-3 mix, variations were 0.33% (length), 1.98% (width), and 0.76% (height). The greatest variation was noted in width, with a maximum of 1.99% in D-3, likely due to the sawdust's tendency to retain moisture, causing slight expansion during curing and subsequent shrinkage during drying. This behavior reflects the material's natural hygroscopic properties, influencing the overall dimensional stability of the blocks. Table 4 shows the dimensional variations of the concrete units used.

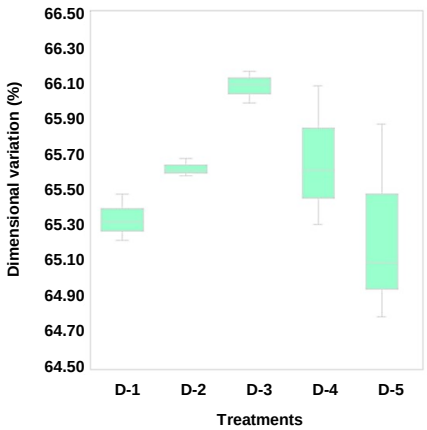

Figure 3 Dimensional variation as a function of sawdust percentage.

Table 4 Dimensional variation in concrete units

Sample description	Dimensional variation						Standard classification
	Length (mm)	V (%)	Width (mm)	V (%)	Height (mm)	V (%)	
D-1 (Standard block)	397.68	0.58	117.86	1.79	198.51	0.74	*NLB
D-2 (5% sawdust)	398.25	0.44	117.62	1.99	198.47	0.77	*NLB
D-3 (10% sawdust)	397.98	0.51	119.73	0.23	198.17	0.91	*NLB
D-4 (15% sawdust)	397.55	0.61	118.43	1.31	198.58	0.71	*NLB
D-5 (20% sawdust)	398.18	0.46	118.59	1.18	198.66	0.67	*NLB

Note: *NLB (Non-load-bearing block)

3.1.2 Warping test

The warping test was conducted using the same number of blocks as in the dimensional variation test, aiming to measure the concavity and convexity of each specimen. As shown in Table 5, the blocks exhibited the greatest warping in a convex form, with a maximum value of 1.70 mm for blocks containing 10% sawdust. This value remains well below the 8 mm limit recommended for non-structural (NP) blocks recommended in the ASTM C426 standard [56]. Notably, there is a lack of references on the specific effects of sawdust on warping behavior in concrete. This highlights the novelty and significance of this study, as it contributes valuable insights into how sawdust influences the physical properties of concrete, particularly regarding dimensional stability and deformation patterns. These findings can serve as a reference for future research in the development of eco-friendly construction materials.

Table 5 Warping on the top and bottom faces of masonry blocks

Sample description	Top face (mm)		Bottom face (mm)	
	Concave	Convex	Concave	Convex
D-1 (Standard block)	0.74	1.58	0.78	1.62
D-2 (5% sawdust)	0.71	1.55	0.55	1.67
D-3 (10% sawdust)	0.85	1.41	0.35	1.70
D-4 (15% sawdust)	0.58	1.52	0.73	1.56
D-5 (20% sawdust)	0.57	1.43	0.66	1.44

3.1.3 Absorption test

In Figure 4, the ANOVA test yielded a significance value of 3.69e-06, which is less than 0.05, indicating a statistically significant difference between treatments. Additionally, Tukey's multiple comparisons test identified treatment D-5 (20% sawdust) as having the highest absorption rate. The standard block showed an absorption percentage of 8.89%, while the absorption increased progressively with higher sawdust content. The increase in water absorption observed in Figure 4 is attributed to the porous nature of sawdust, which introduces additional voids within the concrete matrix. As the sawdust content increases, these voids create capillary channels that enhance water retention. Treatment D-5 (20% sawdust) showed the highest absorption (12.04%) due to its higher organic content, leading to reduced material density and greater permeability. This linear trend highlights sawdust's hydrophilic properties, significantly influencing moisture uptake compared to the standard block.

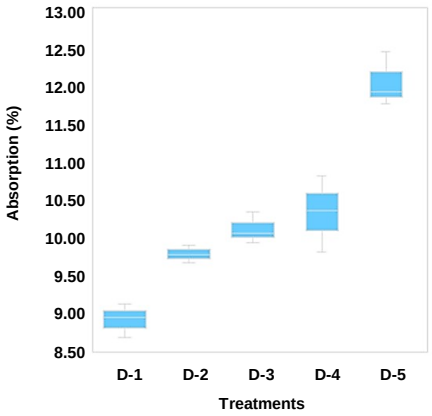

Figure 4 Variation of the absorption test as a function of the percentage of sawdust.

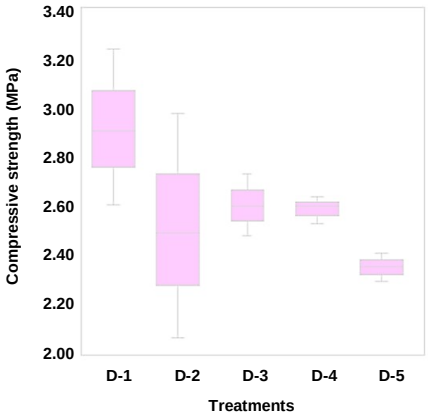

Figure 5 Variation of compressive strength of blocks at 28 days as a function of the percentage of sawdust.

3.2 Mechanical properties of concrete hollow blocks

3.2.1 Compressive strength test

In Figure 5, the ANOVA test resulted in a p-value of 0.184 (> 0.05), indicating no statistically significant difference among the treatments. This conclusion is supported by Tukey's multiple comparison test.

The standard block (D-1) exhibited the highest average compressive strength of 2.92 MPa. The incorporation of 5%, 10%, 15%, and 20% sawdust resulted in reductions of 2.51 MPa (14.04%), 2.60 MPa (10.95%), 2.59 MPa (11.30%), and 2.35 MPa (19.52%), respectively, compared to the standard block. These reductions are attributed to the weaker bonding between sawdust particles and the cement matrix, leading to the formation of microcracks and increased porosity, which negatively affect compressive strength. Despite the reductions, 10% sawdust remains acceptable as it provides a balance between sustainability and structural performance, suggesting its potential for use in non-load-bearing applications.

3.2.2 Compressive strength testing of masonry piles

The prisms evaluated at 28 days, composed of two hollow blocks with a 1:4 mortar ratio, showed a trend of decreasing compressive strength (f'm) as the sawdust content increased. The standard block had an f'm of 9.58 MPa, while reductions of 4.73% (9.13 MPa), 5.85% (9.02 MPa), and 6.30% (8.98 MPa) were observed for 10%, 15%, and 20% sawdust, respectively. Interestingly, prisms with 5% sawdust (D-2) exhibited an 8.59% increase, reaching 10.40 MPa, surpassing the standard block.

According to Figure 6, the ANOVA test showed a significant difference between treatments ($p = 0.00352 < 0.05$). Tukey's test indicated that both the standard block (D-1) and D-2 maximized compressive strength without significant differences (both labeled "a"). D-2 (5% sawdust) had the highest compressive strength, confirming its potential for sustainable masonry applications.

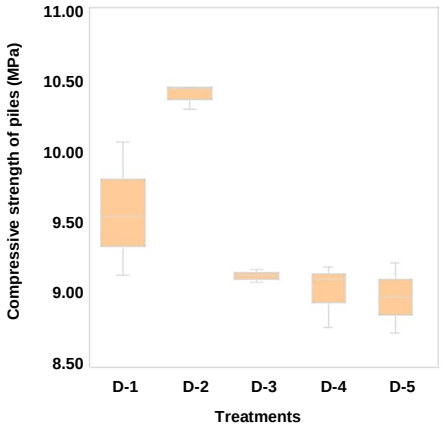

Figure 6 Variation of the compressive strength in piles at 28 days as a function of the percentage of sawdust.

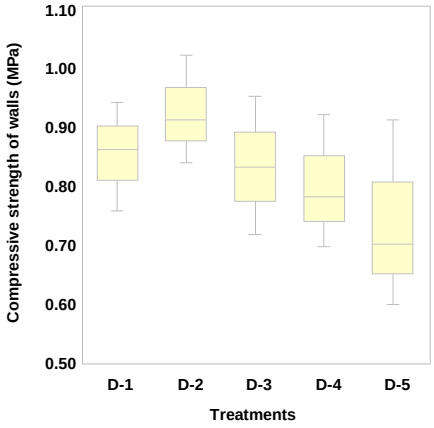

Figure 7 Variation of compressive strength in walls at 28 days as a function of the percentage of sawdust.

3.2.3 Diagonal compressive strength test on masonry walls

The compressive strength results, adjusted for standard deviation based on the average values of each design, were 0.89, 0.94, 0.88, 0.86, and 0.85 MPa, respectively, compared to the standard block. Walls incorporating 10%, 15%, and 20% sawdust showed compressive strength reductions of 0.00%, 6.05%, and 8.35%, respectively, relative to the control walls. Despite these reductions, treatment D-2 (5% sawdust) demonstrated the highest compressive strength, with a sample average of 0.94 MPa.

According to Figure 7, the ANOVA test produced a p-value of 0.427 (> 0.05), indicating no statistically significant differences between treatments overall. This suggests that sawdust incorporation up to 20% does not cause significant variations in the diagonal compressive strength of masonry walls under these test conditions, although the highest average strength was observed with the 5% sawdust addition (D-2).

3.2.4 X-ray diffraction (XRD)

Figure 8 presents X-ray diffraction diffractograms showing the crystalline phases of the standard concrete and concrete with the addition of 10% sawdust. The figure shows an X-ray diffraction (XRD) pattern comparing the crystalline phases of a standard concrete material (black line) and concrete containing 10 % sawdust (red line). The x-axis represents the diffraction angle (2θ, degrees), and the y-axis indicates the intensity (counts), reflecting the abundance of crystalline phases. Table 6 details the concentration of crystalline and amorphous phases by the Reference Intensity Ratio (RIR) technique for the standard block and the concrete with 10% sawdust.

It is observed that the control concrete has a concentration of 26.9% quartz and the concrete with 10% sawdust has 27.6% quartz, highlighting these crystalline phases for their higher concentration. The XRD pattern reveals that incorporating sawdust modifies the concrete's mineralogical composition, reducing dominant phases like quartz while promoting secondary phases such as ettringite and nahcolite. This shift affects the material's mechanical properties and durability.

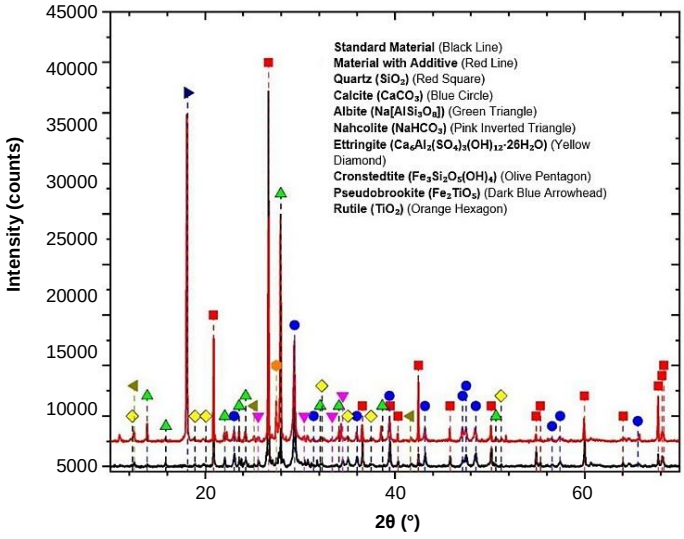

Figure 8 X-ray diffractogram of standard block and block with 10% sawdust.

Table 6 Crystalline phase concentration in standard and 10% sawdust concrete by RIR.

Crystalline Phase	Formula	According to database number	Concentration Standard concrete (% in weight)	Concrete with 10% sawdust (% in weight)
Quartz	SiO_2	46 - 1045	26.9	27.6
Calcite	$CaCO_3$	89 - 6424	19.8	20.8
Albite	Na $[AlSi_3O_8]$	05 - 0586	19.5	8.5
Rutile	TiO_2	65 - 1118	--	3.2
Nahcolite	$NaHCO_3$	15 - 0700	7.5	9.2
Ettringite	$Ca_6Al_2(SO_4)_3(OH)_{12}26H_2O$	41 - 1451	2.3	2.3
Cronstedtite	$Fe_3Si_2O_5(OH)_4$	72 - 1675	1.2	1.6
Pseudobrokite	Fe_2TiO_5	76 - 1743	--	1.5
Amorphous	--	--	22.8	24.7

3.2.5 Scanning Microscopy SEM-EDS

Figure 9 (Top) displays micrographs of the standard uncrushed concrete at 500X and 2000X magnifications, revealing a homogeneous, dense, and low-porosity cement matrix, indicating strong bonding and compactness. In contrast, Figure 9 (Bottom) shows micrographs of the powder form standard block at the same magnifications, highlighting slight changes in texture due to mechanical crushing. Additionally, Figure 10 presents the EDS spectrum, identifying the chemical elements present in the standard concrete sample. The analysis confirms a well-distributed composition of key elements such as calcium, silicon, and oxygen, which contribute to the material's structural integrity.

When compared to the standard block with 10% sawdust, the images reveal a less uniform microstructure with increased porosity and irregular voids. This is attributed to the heterogeneous distribution of sawdust particles, which disrupts the compactness of the cement matrix, potentially influencing mechanical properties like strength and water absorption.

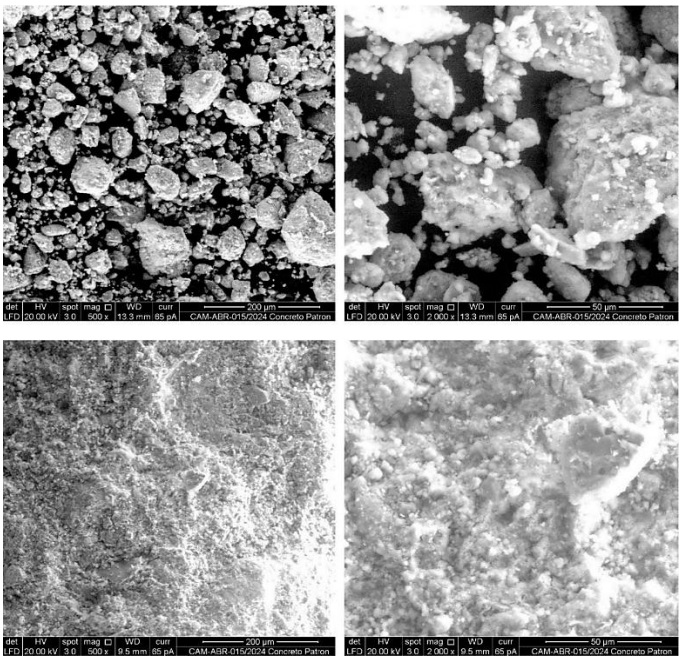

Figure 9 Micrographs of the standard sample at 500X and 2000X magnifications.

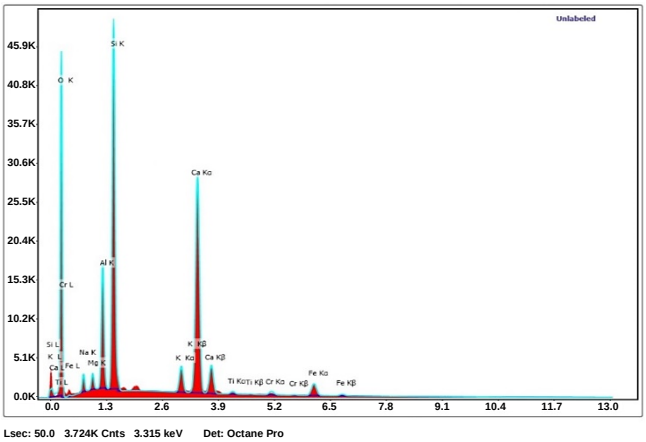

Figure 10 EDS spectra of the standard block sample.

Figure 11 shows micrographs of the standard concrete block sample with sawdust additive in powder form (top) and uncrushed (bottom) at 500X and 2000X magnifications. In addition, Figure 12 presents the EDS spectra showing the adjustment and the elements for the analysis of the chemical composition of the standard block + 10% sawdust sample. In these images, the micromorphology of the standard block with 10% sawdust can be observed, which shows a more porous and less dense cement matrix compared to the standard block, showing a less uniform distribution due to the added sawdust.

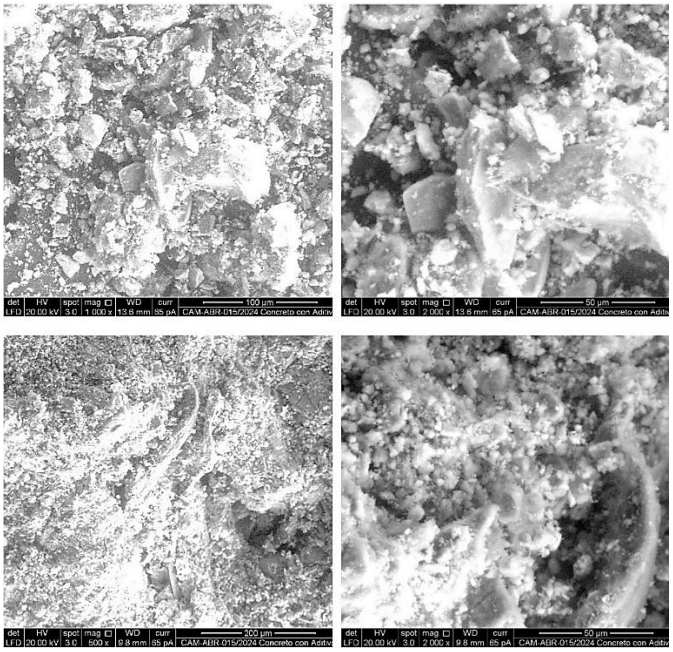

Figure 11 Micrographs of 10% sawdust sample at 500X and 2000X magnification.

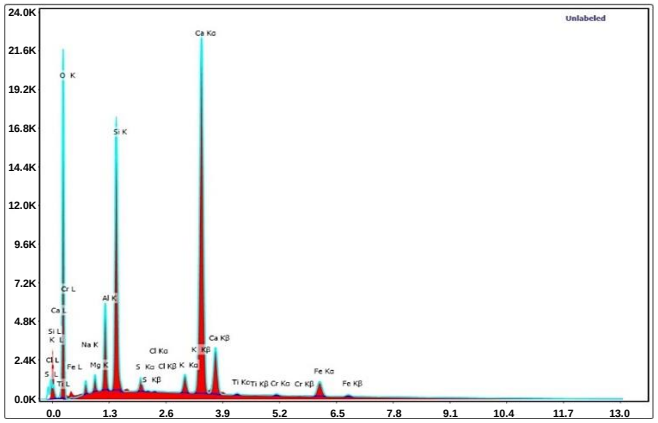

Figure 12 EDS spectra of the sample with 10% sawdust

Table 7 EDS chemical composition of standard block and 10% sawdust sample.

Chemical element	Standard block		10% sawdust	
	*wt%	**at%	*wt%	**at%
C	7.10	11.82	8.15	13.63
O	49.57	61.97	49.62	62.30
Na	1.49	1.29	1.01	0.88
Mg	0.77	0.63	0.72	0.60
Al	5.08	3.77	3.15	2.34
Si	13.97	9.95	8.75	6.26
S	--	--	0.55	0.34
Cl	--	--	0.05	0.03
K	1.59	0.81	0.93	0.48
Ca	17.02	8.50	23.86	11.96
Ti	0.29	0.12	0.17	0.07
Cr	0.54	0.21	0.26	0.10
Fe	2.59	0.93	2.78	1.00

*wt% (weight percent); **at% (atomic percent)

Table 7 presents the EDS chemical composition of standard block and block with 10% sawdust. The standard concrete shows a higher silicon content (13.97 wt%) compared to the sawdust sample (8.75 wt%), indicating reduced silicate phases. In contrast, calcium

increased from 17.02 wt% to 23.86 wt% with sawdust, suggesting enhanced calcium-based compounds. Carbon content also rose, likely due to organic material from sawdust. Minor elements like Na, Al, and K decreased, reflecting compositional changes influenced by sawdust addition.

4. Discussions

4.1 Dimensional variation test

These variations in none of the cases exceed the variations recommended in ASTM 140 [55]; on the other hand, Shantveerayya et al. [33] similarly found greater variation in their hollow blocks with respect to their height, obtaining a result of 6.04%, in a handmade manufacturing method, as for the incorporation of sawdust, Table 4 indicates its variation in different dimensions.

4.2 Absorption test

These findings are similar by Boob [34], who obtained an increase in their absorption values in their bricks with recycled concrete and sawdust, are for a combination of 80% sand and 15% sawdust obtained a value of 6.25% absorption; similarly, Abera [35], finds that there is an increase in absorption values reaching 11. In addition, the results obtained by Abed and Khaleel [37], are the most similar to the present study in terms of numerical value, reaching the maximum absorption value of 16.25%, however, there is a tendency to increase as the sawdust content increases.

4.3 Compressive strength test

This finding coincides with the replacement percentages of 15% sawdust, where they obtained the best compressive strength compared to the standard block [38]; on the other hand, in terms of compressive strength with 4% sawdust increased the strength, however, it decreased by 6. 48% with respect to the standard block [35], similar to the present research, a significant increase in the f'b of concrete blocks has been found with respect to the other designs for the addition of 10% sawdust, but at the same time it decreases by 7.5% with respect to standard blocks at 28 days [31], the results obtained in the present research the one that stands out the most with respect to the other designs are the same with 10% sawdust, which decreases by 1.85%.

4.4 Compressive strength testing of masonry piles

These results are similar to those found in other studies, but differ from the general trend where f'm values are usually lower than f'b values by up to 31% [32]. This discrepancy can be attributed to several factors, such as the shape of the block, the strength of the mortar used, or the width/height ratio of the prisms. According to ASTM 1314 [58], load-bearing blocks should have f'm values between 7.3 and 11.8 MPa. In this study, all the prisms produced comply with these established values, reaching the required strength.

4.5 Diagonal compressive strength test on masonry walls

A similar trend is seen in the shear strength test of brick masonry with sawdust addition, which despite testing different classes of cement-lime mortar, the strength of the walls decreased as the proportion of sawdust in the bricks increased [32]. The tested walls showed diagonal failures, indicating good adhesion of the mortar to the blocks. The V'm values for each design conform to the recommended range for non-bearing blocks (0.8 to 1.1 MPa) according to ASTM E519 [59], suggesting the feasibility of hollow concrete blocks with sawdust as non-bearing blocks.

4.6 X-ray diffraction (XRD)

These results are in agreement with the findings of Muñoz Pérez et al. [17], who by X-ray diffraction identified a high concentration of quartz, albite and other similar crystalline phases, and the predominant presence of silica and portlandite highlighted the crucial role of these minerals in the composition of the concrete. Similarly, Muñoz Pérez et al. [41], observed albite, quartz and orthoclase, in addition to an amorphous phase, in their analysis, and the concrete showed a significant concentration of quartz (34.5%), along with lower amounts of albite, microcline and other phases. The amorphous phase reached 20.2%, suggesting that, as in previous studies, the presence of crystalline silica and amorphous components may influence the strength of concrete. These results underscore the importance of less reactive crystalline phases and the amorphous phase in improving the performance of concrete in structural applications.

4.7 Scanning Microscopy SEM-EDS

This observation is consistent with the findings of Agrawal et al. [45], who reported that concrete with residues showed the presence of Ca, O and Si in similar atomic percentages. Similarly, Adeboje et al. [44], detected 19.44% C, 8.28% O, 0.63% Si, 49% Fe, 14.04% Cl and 7.05% Ni, which is in agreement with the results of this study as the same chemical elements were found. In this context, the SEM image of concrete with 10% sawdust suggests that, although the addition of this type of aggregate improves the uniformity of the structure and reduces the porosity, the effects may vary according to the proportions and type of sawdust used.

5. Conclusions

This study analyzes the physical (dimensional variation, warping, absorption), mechanical (compressive strength, prism compression and diagonal compression of walls) and microstructural (X-ray diffraction, material characterization by scanning electron microscopy) properties of hollow standard block with a sawdust incorporating of 5, 10, 15 and 20%, with the following conclusions:

Regarding the physical properties of standard and experimental concrete blocks, it was determined that both dimensional variation and warping of the blocks did not show significant variations in any of the designs. In addition, the standard blocks presented an

absorption percentage of 8.98%. This absorption progressively increased as the sawdust content increased, probably due to the high porosity of the sawdust.

The incorporation of sawdust reduced the mechanical properties of concrete blocks, with a linear decrease as the sawdust percentage increased. The standard block showed 2.91 MPa strength and 9.59 MPa axial resistance. This reduction is attributed to weak bonding between sawdust and the cement matrix, causing microcracks. Failures appeared as vertical cracks in piles and diagonal in walls, indicating good mortar-block adhesion despite strength loss.

The optimum sawdust addition is 10%, with a compressive strength of 2.60 MPa, meeting the design requirement of 1.94 MPa. Design D-3 (10% sawdust) qualifies as load-bearing, while D-2 (5%), D-4 (15%), and D-5 (20%) are non-load-bearing, complying with ASTM standards. Sawdust proves to be an effective admixture for sustainable concrete block manufacturing, enhancing eco-friendly construction practices

The results of the XRD analysis reveal that both the standard concrete sample and the concrete sample with 10% sawdust are composed mainly of silicates, silicon dioxides and calcium dioxide. Additionally, an amorphous phase was identified that could not be detected by XRD. The EDS analysis showed a high content of carbon, oxygen, aluminum, silicon and calcium, in addition to the presence of several other elements in smaller proportions.

This research contributes to the Sustainable Development Goals (SDGs), particularly SDG 9 (Industry, Innovation, and Infrastructure), by promoting the use of alternative materials in construction; SDG 11 (Sustainable Cities and Communities), by encouraging more sustainable buildings; and SDG 12 (Responsible Consumption and Production), by fostering the valorization of waste materials such as sawdust in the construction industry.

For future research, it is recommended to conduct acoustic performance tests, given the potential of sawdust to improve sound insulation due to its fibrous structure. Additionally, durability assessments, including thermal insulation, long-term weathering, and fire resistance tests, will provide a comprehensive understanding of the material's behavior in diverse environmental conditions.

6. Acknowledgments

The authors wish to thank the SEIMSUP laboratory and LEMS W&C EIRL for the support provided in carrying out the tests required for the development of the research.

7. References

[1] Syamsiyah NR, Mutiari D, Arsandrie Y, Suharyani, Himmah SA. Acoustic performance from a mixture of plastic waste, wood dust, and rice husk. Civ Eng Archit. 2020;8(4):490-9.
[2] Supar K, Rani FAA, Mazlan NL, Musa MK. Partial replacement of fine aggregate using waste materials in concrete as roof tile: a review. IOP Conf Ser: Mater Sci Eng. 2021;1200:012008.
[3] Thakur A, Kasilingam S, Singh AP. Evaluation of concrete bricks with crumb rubber and polypropylene fibres under impact loading. Constr Build Mater. 2022;315:125752.
[4] Raheem AA, Ikotun BD. Incorporation of agricultural residues as partial substitution for cement in concrete and mortar – a review. J Build Eng. 2020;31:101428.
[5] Burgos Cotrina JA, Cubas Benavides EA, Garcia Chumacero JM. Analysis of the combination of glass and polypropylene fibers on the mechanical properties of mortar. J Build Pathol Rehabil. 2025;10:22.
[6] Omar MF, Abdullah MAH, Rashid NA, Abdul Rani AL. Partially replacement of cement by sawdust and fly ash in lightweight foam concrete. IOP Conf Ser: Mater Sci Eng. 2020;743:012035.
[7] De la Cruz Carlos MB, Jiménez Revilla WE, García Chumacero JM, Muñoz Pérez SP, Villegas Granados LM. Influence of sawdust on the mechanical behavior of C28 concrete containing ground glass. Innov Infrastruct Solut. 2024;9:433.
[8] Burga Bustamante G, Muñoz Pérez SP, García Chumacero JM, Sánchez Diaz E, Ruiz Pico AA, Rodriguez Laffite ED, et al. Evaluation of the mechanical behavior of concrete with the addition of dry corn fiber. Innov Infrastruct Solut. 2025;10:29.
[9] Dawood ET, Mahmood MS. Production of sustainable concrete brick units using nano-silica. Case Stud Constr Mater. 2021;14:e00498.
[10] Kilani A, Olubambi A, Ikotun B, Oladejo OS, Famodimu B. Evaluating the reinforcements efficiency of sawdust and corncob wastes in structural concrete: a comprehensive review. J Build Mater Struct. 2023;10:40-63.
[11] Mwango A, Kambole C. Engineering characteristics and potential increased utilisation of sawdust composites in construction—a review. J Build Constr Plan Res. 2019;7(3):59-88.
[12] Raavi SSD, Tripura DD. Predicting and evaluating the engineering properties of unstabilized and cement stabilized fibre reinforced rammed earth blocks. Constr Build Mater. 2020;262:120845.
[13] Meko B, Ighalo JO. Utilization of *Cordia Africana* wood sawdust ash as partial cement replacement in C 25 concrete. Clean Mater. 2021;1:100012.
[14] Sharba AAK, Hason MM, Hanoon AN, Qader DN, Amran M, Abdulhameed AA, et al. Push-out test of waste sawdust-based steel-concrete – steel composite sections: experimental and environmental study. Case Stud Constr Mater. 2022;17:e01570.
[15] Opiso EM, Supremo RP, Perodes JR. Effects of coal fly ash and fine sawdust on the performance of pervious concrete. Heliyon. 2019;5(11):e02783.
[16] Jeyashree TM, Somesh MS. Characteristic study on concrete elements using agro-waste as a replacement of fine aggregate. Res Eng Struct Mater. 2023;9(4):1255-66.
[17] Muñoz Pérez SP, Sánchez Díaz E, Barboza-Cullqui D, García-Chumacero JM. Use of recycled concrete and rice husk ash for concrete: a review. J Appl Res Technol. 2024;22(1):138-55.
[18] Muñoz Pérez SP, Santisteban Purizaca JF, Castillo Matute SM, García Chumacero JM, Sánchez Diaz E, Diaz Ortiz EA, et al. Glass fiber reinforced concrete: overview of mechanical and microstructural analysis. Innov Infrastruct Solut. 2024;9:116.
[19] Vasquez Diaz NA, Ruiz Meza AF, García Chumacero JM, Villegas Granados LM. Influence of treated and purified wastewater with biofilter on the strength and durability of concrete. Innov Infrastruct Solut. 2025;10:134.
[20] Chapoñan Inoñan JJ, Delgado Fernández E, Muñoz Pérez SP, Garcia Chumacero JM, Sánchez Diaz E, Diaz Ortiz EA, et al. Influence of polypropylene fibers on the microstructure and physical and mechanical properties of concrete. Innov Infrastruct Solut. 2024;9:488.

[21] Vallejos J, Montenegro M, Muñoz S, García J. Mechanical and microstructural properties of environmentally friendly concrete partially replacing aggregates with recycled rubber and recycled PET. J Sustain Archit Civil Eng. 2024;36(3):94-110.
[22] García Chumacero JM, Gonzales Macedo JL, Sánchez Castillo DJ. Contribution of agricultural ashes and HDPE as a waste material for a sustainable environment applied to the stabilization of a low plasticity clay soil. Innov Infrastruct Solut. 2024;9:67.
[23] García J, Arriola G, Villena L, Muñoz S. Strength of concrete using partial addition of residual wood ash with respect to cement. Rev Politéc. 2023;52(1):45-54.
[24] Muñoz Perez SP, Garcia Chumacero JM, Charca Mamani S, Villena Zapata LI. Influence of the secondary aluminum chip on the physical and mechanical properties of concrete. Innov Infrastruct Solut. 2023;8:45.
[25] Muñoz S, Villena L, Tesen F, Coronel Y, Garcia J, Brast C. Influence of coconut fiber on mortar properties in masonry walls. Electron J Struct Eng. 2023;23(4):52-8.
[26] Bereche J, García J. Replacement of fine aggregate with refractory brick residue in concrete exposed to elevated temperatures. Rev Politéc. 2024;53(2):79-88.
[27] Muñoz Pérez SP, Pardo Becerra JM, García Chumacero JM, Sánchez Diaz E, Diaz Ortiz EA, Rodriguez Laffite ED, et al. Evaluation of the physical and mechanical properties of concrete with the incorporation of recycled concrete aggregate. Innov Infrastruct Solut. 2024;9:204.
[28] Garcia Chumacero JM, Acevedo Torres PL, Corcuera La Portilla CC, Muñoz Perez SP, Villena Zapata LI. Effect of the reuse of plastic and metallic fibers on the characteristics of a gravelly soil with clays stabilized with natural hydraulic lime. Innov Infrastruct Solut. 2023;8:185.
[29] Chaname J, García J, Arriola G. Improvement of the mechanical properties of structural concrete using microporous ethylene vinyl acetate. Rev Politéc. 2024;53(2):17-26.
[30] Ekhuemelo DO, Gbaeren ET, Tembe ET. Evaluation of lime treated mixed sawdustas fractional replacement for sand in the production of sandcrete hollow blocks. Int J Sci Eng Investig. 2017;6(65):21-7.
[31] Assiamah S, Agyeman S, Adinkrah-Appiah K, Danso H. Utilization of sawdust ash as cement replacement for landcrete interlocking blocks production and mortarless construction. Case Stud Constr Mater. 2022;16:e00945.
[32] Raheem AA, Sulaiman OK. Saw dust ash as partial replacement for cement in the production of sandcrete hollow blocks. Int J Eng Res Appl. 2013;3(4):713-21.
[33] Shantveerayya K, Mahesh Kumar CL, Shwetha KG, Jima F, Fufa K. Performance evaluation of hollow concrete blocks made with sawdust replacement. Int J Eng. 2022;35(6):1119-26.
[34] Boob TN. Performance of saw-dust in low cost sandcrete blocks. Am J Eng Res. 2014;3(4):197-206.
[35] Abera MA. Investigating the acceptable quantity of fine aggregate to be replaced with sawdust to obtain strong, light weight, and economical result for HCB production. Int J Adv Res Ideas Innov Technol. 2019;5(5):391-5.
[36] Garcia Chumacero WR, Garcia Chumacero JM, Muñoz Perez SP, Chávez Cotrina CO, Villegas Granados LM. Use of secondary aluminum slag powder on the strength of non-load-bearing lightweight concrete blocks. Civ Eng Archit. 2024;12(6):3733-41.
[37] Abed JM, Khaleel BA. Effect of wood waste as a partial replacement of cement, fine and coarse aggregate on physical and mechanical properties of concrete blocks units. Int J Integr Eng. 2019;11(8):229-39.
[38] Dominguez-Santos D. Structural performance of concrete blocks with wood aggregates for the construction of medium and high-rise buildings. Informes de la Construcción. 2021;73(564):e414. (In Spanish)
[39] Dadzie DK, Dokyi GO, Niakoh N. Comparative study of the properties of sandcrete blocks produced with sawdust as partial replacement of sand. Int J Sci Eng Res. 2018;9(3):1357-63.
[40] Dominguez-Santos D, Mora-Melia D, Pincheira-Orellana G, Ballesteros-Pérez P, Retamal-Bravo C. Mechanical properties and seismic performance of wood-concrete composite blocks for building construction. Materials. 2019;12(9):1500.
[41] Muñoz Pérez SP, Charca Mamani S, Villena Zapata LI, Leiva Piedra JL, Gonzales Ayasta S, Rodriguez Lafitte ED, et al. Infuence of rice husk ash (RHA) with gypsum and ichu fbers in the processing of geopolymers. Innov Infrastruct Solut. 2023;8:211.
[42] Meena RV, Jain JK, Chouhan HS, Beniwal AS. Use of waste ceramics to produce sustainable concrete: a review. Clean Mater. 2022;4:100085.
[43] Guo J, Huang M, Huang S, Wang S. An experimental study on mechanical and thermal insulation properties of rubberized concrete including its microstructure. Appl Sci. 2019;9(14);2943.
[44] Adeboje AO, Kupolati WK, Sadiku ER, Ndambuki JM. Influence of partial substitution of sand with crumb rubber on the microstructural and mechanical properties of concrete in Pretoria, South Africa. Int J Environ Waste Manag. 2019;24(1):39-60.
[45] Agrawal D, Waghe U, Ansari K, Dighade R, Amran M, Qader DN, et al. Experimental effect of pre-treatment of rubber fibers on mechanical properties of rubberized concrete. J Mater Res Technol. 2023;23:791-807.
[46] ASTM. ASTM C136-06: Standard test method for sieve analysis of fine and coarse aggregates. West Conshohocken: ASTM International; 2015.
[47] ASTM. ASTM C29: Standard test method for bulk density (“unit weight”) and voids in aggregate. West Conshohocken: ASTM International; 2017.
[48] ASTM. ASTM C127: Standard test method for relative density (specific gravity) and absorption of coarse aggregate (withdrawn 2024). West Conshohocken: ASTM International; 2024.
[49] ASTM. ASTM C566: Standard test method for total evaporable moisture content of aggregate by drying. West Conshohocken: ASTM International; 2019.
[50] Cabanillas Hernandez G, García Chumacero JM, Villegas Granados LM, Arriola Carrasco GG, Marín Bardales NH. Sustainable use of wood sawdust as a replacement for fine aggregate to improve the properties of concrete: a Peruvian case study. Innov Infrastruct Solut. 2024;9:233.
[51] Cadenas Alvarado LY, Jacinto Huamanchumo RM, Garcia Chumacero JM, Salinas Vásquez NR, Chavez Cotrina CO. Experimental study of hybrid concrete blocks based on sawdust and calcined clay using cement as a binder. Innov Infrastruct Solut. 2024;9:445.
[52] Reglamento Nacional de Edificaciones. Propuesta de NORMA E.070 “ALBAÑILERÍA”. Lima: SENCICO; 2019. (In Spanish)
[53] Ministerio de Vivienda, Construcción y Saneamiento. Comentarios A La Norma Técnica de Edificación E.070 “Albañilería”. Lima: SENCICO; 2008. (In Spanish).
[54] ACI. ACI 211.1: Standard practice for selecting proportions for normal, heavyweight, and mass concrete. United States: ACI; 2022.

[55] ASTM. ASTM C140-13: Standard test methods for sampling and testing concrete masonry units and related units. West Conshohocken: ASTM International; 2013.
[56] ASTM. ASTM C426-22: Standard test method for linear drying shrinkage of concrete masonry units. West Conshohocken: ASTM International; 2023.
[57] ASTM. ASTM C307-18: Standard test method for tensile strength of chemical-resistant mortar, grouts, and monolithic surfacings. West Conshohocken: ASTM International; 2023.
[58] ASTM. ASTM C1314-22: Standard test method for compressive strength of masonry prisms. West Conshohocken: ASTM International; 2022.
[59] ASTM. ASTM E519: Standard test method for diagonal tension (shear) in masonry assemblages. West Conshohocken: ASTM International; 2020.